J. Fluid Mech. (1971), *vol.* 45, *part* 3, *pp.* 545–559
Printed in Great Britain

On stationary and travelling vortex breakdowns

By TURGUT SARPKAYA

Department of Mechanical Engineering, Naval Postgraduate School, Monterey, California

(Received 29 December 1969 and in revised form 15 June 1970)

This paper describes some experiments in swirling flows in a diverging cylindrical tube in which various types of vortex breakdowns were observed.

In one set of experiments, the position of the breakdown, axial component of the velocity of the vortex core, swirl angle distribution ahead of the breakdown, and the pressure distribution along the tube were determined for various flow rates and for various values of circulation imparted to the fluid (water). Basically, three types of vortex breakdown were observed, viz. mild (double helix) breakdown, spiral breakdown (followed by turbulent mixing), and axisymmetric breakdown (followed by a thicker vortex core, then a spiral breakdown, and finally by turbulent mixing). The type and the location of the stationary breakdowns were found to be dependent, for the particular vortex tube used, upon the Reynolds and circulation numbers of the flow. In a spiral breakdown, the vortex core filament maintained the *same* sense of rotation as the upstream fluid elements. In an axisymmetric breakdown, the bubble included an inclined vortex-ring whose axis gyrated about the axis of the tube.

In a second set of experiments, the response of the abrupt structural change along the axis of flow to gradual and abrupt changes in the upstream and downstream flow conditions was examined. The axisymmetric breakdown responded in a manner analogous to the hydraulic jump in open-channel flow before if reached a new stationary position along the axis of the tube.

The observations reported and the evidence presented herein revealed that the axisymmetric breakdown is a finite transition between two sequent states of flow as proposed by Benjamin (1962, 1965, 1967) on theoretical grounds.

1. Introduction and review of existing information

Since the discovery of the vortex breakdown phenomenon (an impressive structural change, generally liable to occur in any flow characterized by longitudinal vortices), many theoretical and experimental studies have been conducted. The difficulties, both mathematical and experimental, involved in describing the nature, predicting the location, and identifying the occurrence of the phenomenon have been well documented (see, for example, Hall 1966*a*, p. 53 *et seq.*).

Vortex breakdown has been observed to occur over delta wings at large incidences and in axisymmetric swirling flows in tubes. In either case, different intermediate forms, between two extreme types of breakdown have been

recognized. In the periodic spiral type of breakdown, the axial filament is deformed into a spiral configuration following an abrupt kink at a point slightly ahead of the apparent stagnation point. The sense of the spiral, according to the observations of Lambourne & Bryer (1962) on delta wings, is *opposite* to the direction of rotation of the ambient flow (a result contrary to the observations reported herein for a confined flow). In the nearly steady and axisymmetric type of breakdown, a dyed filament of fluid along the axis of the core appears to spread symmetrically from the stagnation point and to enclose a quasi-stationary structure referred to as a 'bubble'. According to Harvey (1962), "the flow downstream of the bubble showed no signs of a reversed core, but appeared rather to have returned to a form similar to that upstream of the breakdown".

Of the two forms of breakdown cited above, the spiral type is more commonly observed over a delta wing while the axisymmetric type generally appears in an axisymmetric swirling flow.

The existence of these phenomena and other related observations to be described later, has considerable bearing upon the relative merits of various theoretical predictions regarding the nature and causes of vortex breakdown. According to Lowson (1964) and Jones (1964), the phenomenon, attendant to leading-edge vortices, always commences as a spiralling of the axial filament while the axisymmetric form is a later development of the primary spiral form. Lambourne (1965) presented experimental evidence to the contrary and argued that the breakdown is initially axisymmetric but becomes unstable and finally changes into the spiral form. He suggested that the theory should first seek to explain the axisymmetric form and then discover the conditions under which it may degenerate into a spiral form. According to Ludwieg (1962, 1964) and Jones (1960, 1964), the stagnation of leading-edge vortices follows from a hydrodynamic instability of the vortex core with respect to spiral disturbances. Consequently, these investigators maintain that the breakdown ultimately exhibits the spiral form rather than the axisymmetric configuration.

Benjamin (1962, 1965, 1967) considered vortex breakdown as fundamentally a transition, akin to the hydraulic jump, from a uniform state of swirling flow (supercritical) to one (subcritical) featuring axisymmetric standing waves of finite amplitude. His analysis was restricted to 'weak' non-dissipative transitions since it dealt exclusively with the flow of an effectively inviscid fluid which contained vorticity. As pointed out by Benjamin (1965, p. 518), however, the results are not restricted to non-dissipative transitions since even the transitions involving substantial energy dissipation may still be regarded as a finite transition by virtue of the conservation of mass and momentum.

To date, there has not been a crucial test which emphatically supports or refutes Benjamin's elegant theory partly because of the difficulty of preserving the axial symmetry of the stationary transitions, and partly because of the difficulty of making quantitative measurements with travelling breakdowns. In fact, no axially symmetric standing waves have yet been observed in vortex cores under which the aforementioned mathematical conditions might be valid. So far, the applicability of Benjamin's theory to axisymmetric vortex breakdown has rested primarily upon the experiments of Harvey (1962). Granger's

(1968) experiments with surges, generated in a bathtub vortex, tended to substantiate the finite transition model for a 'travelling-bore' type of vortex jump. Pritchard (1970) generated solitary waves in a long cylindrical tube and demonstrated that such waves are possible in any swirling flow on which the angular velocity is distributed non-uniformly. Although the proof of the existence of periodic waves of finite amplitude and permanent form still remains as an important gap in the subject, the solitary wave is a necessary part of Benjamin's theory and the demonstration of its existence in swirling flows is an important step towards the acceptance of the finite transition model.

The present investigation was undertaken approximately 2 years ago for the specific purpose of designing and conducting critical experiments with which to examine the merits of the finite transition theory and the dependence of the vortex jump on various flow parameters.

2. Experimental apparatus and procedure

The experimental equipment (see figure 1) consisted of a plexiglass (Perspex) water tank, adjustable swirl vanes, a diverging pipe, a constant head reservoir, a rotameter, and the necessary piping system.

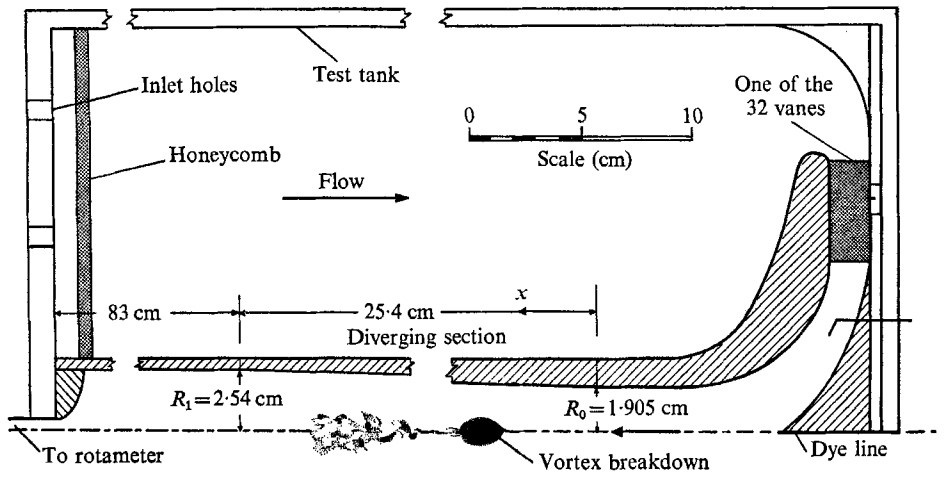

FIGURE 1. Top half of the experimental apparatus.

The inside of the closed test tank was 130 cm long, 35 cm high, and 35 cm wide. The tank was maintained under 8 cm of water pressure by a simple overflow pipe placed in a small Perspex box attached to the top of the tank. One of the end plates (downstream end) contained six inlets which were connected through a larger pipe to the constant head reservoir. Equal amounts of flow were passed through each inlet by properly constricting each supply line leading to the inlet. A honeycomb was placed outside the test pipe and wall-to-wall inside the tank near the inlet holes to further ensure calm flow conditions. The maximum average velocity in the tank, outside the test pipe, was approximately 0·25 cm/sec. The upstream end plate contained two small-bore orifices (0·008 cm) for the passage

of dye. One hole was drilled at the centre of the outer plate, and the other 5 cm above the first. Inside the tank, a second plate was attached to the upstream end plate. A streamlined, conic solid Perspex piece (centre-body) the diameter of which was 16 cm at its base, was fixed to the inner plate. This piece served two purposes. First, it was part of the entrance channel which conveyed the fluid to the diverging test section. Secondly, it contained two small holes (coaxial with the small bore orifices in the outer end plate) for the injection of dye into the flow field. Swirl was imparted to the fluid by 32 streamlined foils (each 3·5 cm long and 2·74 cm wide) placed symmetrically in a circular array around the inlet piece. Each vane was fixed with one screw to the inner plate. A circular ring (1 cm wide, 0·4 cm thick, and 18·5 cm inside diameter) was fitted into the body of the inner plate.† The ring contained 32 small pivots, each one being approximately 0·3 cm long. These pivots were precision fitted to 1·5 cm slots carved in the edge of each vane. With this arrangement, the vane angle was set at any desired value between zero and 60 degrees.‡ The width of the passage between any two vanes changed with the particular vane setting but remained uniform along the passage since the included angle at the tip of each vane was 11·25 degrees (360/32, see figure 2). The average velocity of flow between the vanes $\phi = 60$ degrees, was approximately 7 cm/sec.

As cited above, the streamlined entrance piece (centre-body) attached to the centre of the inner plate constituted part of the channel which conveyed the fluid to the diverging pipe. The outer wall of the channel was formed by another streamlined Perspex piece. It was in turn coupled to the entrance of the diverging tube. This coupling was made in such a manner that there were no protuberances at the junction. The test pipe and the bell-mouth assembly were externally adjustable vertically and laterally (with a wire and screw arrangement between the outer face of the test tube and the tank wall at a section sufficiently far from the vanes). The purpose of this adjustment was to align the dye line (and also the tip of the centre-body) with the axis of the test tube. Failure to do so resulted in the development of an initially spiralling vortex core and attendant spiral disturbances.

The diverging tube, 25·4 cm in length with a 1·905 cm initial radius, constituted the test section. The angle of divergence of the tube was chosen to be 1·434 degrees ($\tan\alpha = 0{\cdot}025$). The bell-mouth joined the diverging test tube through a 5·72 cm long and 1·905 cm radius uniform section which was machined as part of the bell-mouth. A round tube (5·08 cm I.D., and approximately 80 cm long) was smoothly coupled to the downstream end of the test section. The other end of the tube was connected, through a 4 cm long smooth reducer § embedded in the tank wall, to a 2·54 cm I.D. pipe outside the tank. The pipe conveyed the flow to a precision rotameter calibrated for a maximum flow rate of 18 litres per minute.

† This ring could be rotated in its place by means of a simple lever-micrometer mechanism.

‡ Vane angle setting was adjustable to $\frac{1}{120}$ of a degree.

§ The diameter of the exit hole in the reducer was varied from 1 cm to 2·50 cm in 0·5 cm intervals.

The dye injection tubes (one at the axis and the other 5 cm above the axis) were connected to two separate dye reservoirs (containing different colours of dye for colour photography) placed at suitable and easily adjustable elevations. Extreme precautions were taken to ensure the injection of a straight and relatively slow dye filament. A small needle valve on the centre dye-line allowed intermittent dye injection to be accomplished without imparting a flow force on the vortex filament.

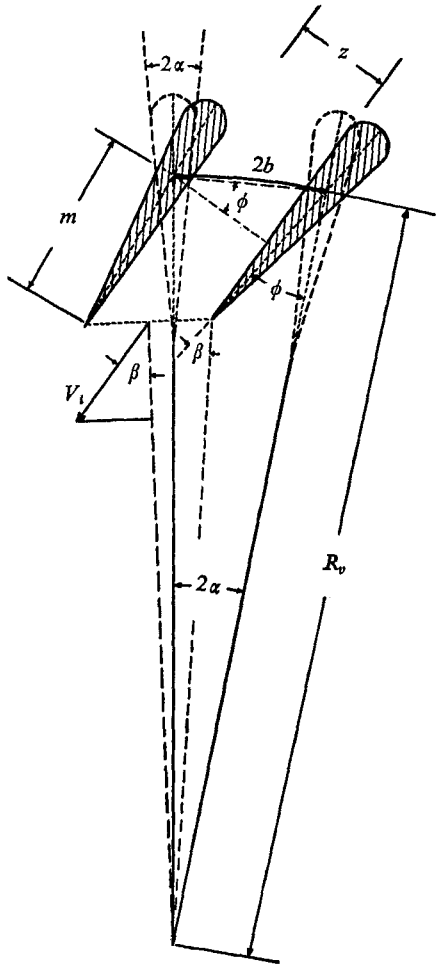

FIGURE 2. Vane geometry and the calculation of circulation number Ω. $R_v = 10{\cdot}65$ cm, $m = 3{\cdot}5$ cm, $w = 2{\cdot}74$ cm (width of vane), $\alpha = 5{\cdot}625°$, $b = \pi R/32$, $z = 2b\cos\phi - 2m\alpha$, $\tan\beta = \sin\phi/(\cos\phi - m/R_v)$, $V_i = Q/32wz$, Q = total flow rate, $\Gamma \cong 2\pi(R_v - m\cos\phi)$ $V_i \sin\beta$, $\Omega = \Gamma/U_0 D_0 = \pi^2 D_0(R_v - m\cos\phi)\sin\beta/64wz$, $D_0 = 2R_0 = 3{\cdot}81$ cm.

Hypodermic tubing (suitably set at the end to an angle radially tangent to a mean surface between the centre-body and the bell mouth) was inserted through the second dye-injection hole. It was moved longitudinally between the two streamlined surfaces in order to visualize streamlines at various radial distances from the axis of the test tube. The hypodermic tubing was first set longitudinally

and then rotated slowly to its final position by comparing the slope of a suitable streamline (made visible by a drop of dye put on one of the vanes) with that of the dye issuing from the tip of the hypodermic tubing. This procedure ensured the injection of the dye filament parallel to the direction of the local streamlines. The maximum Reynolds number of the flow about the hypodermic tubing was approximately 25.

An adjustable mirror covering the total length of the test section and part of the uniform conduit was installed inside the tank to enable the photographing of the top side of the vortex breakdown and the surrounding streamlines. During most of the tests, it was lifted up flush to the inner face of the top cover of the tank. Scale marks engraved at appropriate places on the test pipe and the mirror enabled the extraction of numerical data from the pictures projected on a large screen. Both still and motion pictures (black and white or coloured) were taken with the fluorescent lights permanently placed under and behind the tank. Motion pictures were taken at various constant speeds ranging from 16 to 64 frames per second.†

Attempts to measure the circumferential and axial velocity distributions with a hypodermic tube (connected to a physiological pressure transducer) at a section immediately upstream of the start of the diverging tube were for the most part unsuccessful mainly because the pressure readings were relatively low ($\sim$ 0·5 cm of water). Additionally, the slowness of the response of the small-bore probe to the changes in pressure at various probe locations required an investment of time which was not compatible with the degree of accuracy of the measurements. Instead, one of the test tubes was fitted with wall pressure taps (normal to the bounding surface) located at 1·27 cm intervals along its length. Eight of the pressure taps were monitored simultaneously by connecting them to eight physiological pressure transducers which were in turn connected to a carrier amplifier and digital recorder system. The results yielded temporal mean values and were, as will be discussed later, quite satisfactory.

A hydrogen bubble technique was investigated for velocity distribution determination. It was immediately found that the wire could not be extended across the entire diameter of the tube. When the wire was slowly and radially pushed into the test section while keeping the central dye-injection tube open, the flow pattern outside the core and the breakdown far downstream of the wire remained relatively unaffected until the tip of the wire barely protruded into the vortex core. At this point, a backflow pattern was set up right below the wire, producing an axisymmetric breakdown. When the wire was slowly withdrawn, the flow and the breakdown returned to their previous states. The apparatus was modified so that the wire would only come in from one side of the core and not extend across the entire diameter of the tube. Even then, the pulse timing problems and the buoyancy of the bubbles precluded sufficiently accurate representation of the flow field.

The position of the breakdown, relative to the point where the divergence of the tube started, was determined by setting the vane angle at a desired value and

† Shutter opening angle was 135 degrees. For each film speed, the exposure per frame is thus given by: 135/(360 × film speed).

then changing the flow rate at suitable intervals, or by maintaining the flow rate constant and then systematically altering the vane settings.

3. The observations of the stationary vortex breakdowns

In the first series of experiments, the ratio of the tangential to axial velocity was varied by means of the adjustable vanes while maintaining the flow rate constant.

At a fixed flow rate (say at $Re = 5000$), the dye filament maintained a perfectly straight and laminar form throughout the length of the test tank for a zero-degree vane-angle setting. As the vane angle was slowly increased to 20 degrees, spiralling waves developed toward the end of the uniform tube and the filament became sheared into a tape which broke into turbulence after several revolutions in the form of a helix. As the vane angle was increased to 30 degrees, the filament decelerated rapidly near a point approximately six diameters from the start of the diverging tube, and the filament deformed, following an abrupt kink, into a spiral configuration. The spiral persisted a few turns and then broke into large scale turbulence as seen in figure 3(*a*) (plate 1). The sense of rotation of the spiral was *identical* to that of the fluid surrounding the original filament. An additional small increase in swirl distorted the filament in such a manner that, after the first turn, it developed a tendency to curl back toward the kink as seen in figure 3(*b*) (plate 1). Subsequent increases in swirl resulted in two distinctly different forms of breakdown. The occurrence of either one of these forms depended to a large extent on the rate of increase of swirl and the setting of the centre-body relative to the test tube, i.e. on the upstream disturbances. The first and more commonly observed form (figure 3(*c*), plate 1) is the expansion and folding of the filament, before the completion of the first turn, all the way back to the kink. The subsequent motion of the filament and breakdown into turbulence are clearly visible in figure 3(*c*).

When the filament was perfectly centred, all air bubbles removed from the system, every precaution taken to eliminate internal and external disturbances, and the vane angle was increased extremely slowly (say $\frac{1}{60}$ deg/sec) so as to arrive at the right combination of flow rate and swirl, the original filament rapidly decelerated and expanded into a slightly curved triangular sheet as seen in figure 4 (plate 2). Each half of the continuous sheet wrapped around the other (*rotating in the same sense*) into the form of a double helix. Numerous observations of this type of transition with a slightly-off-centre dye filament have shown that it is highly sensitive to small disturbances, does not envelop a bubble, occurs at relatively low Reynolds and high circulation numbers (at approximately $Re < 2000$ and $\Omega > 2{\cdot}3$), and it gradually expands beyond bounds and breaks up into mild turbulence. These observations strongly suggest that the flow is unstable (in Ludwieg's sense) to spiral disturbances in a region well defined by the Reynolds and circulation numbers and that one of the many possible modes of instability resembles the double-spiral form shown in figure 4.

Further increase of flow produced nearly axisymmetric arrangements as seen in figure 5 (plate 3). The filament did not spread out suddenly and symmetrically

in the form of a 'tulip' but rather maintained its integrity for a short distance on one side of the reversed flow form and then expanded into an undular tape. The entire arrangement was quite unsteady and darted back and forth along the axis, in spite of the fact that both the swirl and flow rate remained constant.

For larger swirls or vane angles, the breakdown form moved progressively upstream and at a definite combination of swirl and flow, the bubble became a smooth and nearly symmetric body, as seen in figure 6 (plate 4). The original filament spiralled about the body (sometimes penetrating it, possibly due to inertia effects related to the slight density difference between the dye and water) and near the downstream end expanded into a triangular tape, part of which spiralled rapidly into the bubble with the remainder spiralling about a relatively larger filament shed from a portion of the vortex ring trapped in the bubble. After a distance of approximately one bubble length, the new core deflected, following an abrupt kink, into a loose spiral configuration. This spiral seldom formed another bubble, possibly due to the instabilities just described, and after a few turns broke into large-scale turbulence.

The axis of the vortex ring gyrated at a regular frequency about the axis of the tube. The fluid in the bubble was replenished from the side of the bubble nearer the downstream portion of the ring and emptied from the side farther from the upstream portion of the ring (see lower photo in figure 6, plate 4). This simultaneous filling and emptying process, possibly due to pressure instabilities in the wake of the bubble, resulted in a new vortex core downstream of the bubble which behaved like a gyroscope precessing about the axis of the tube with a rate of precession equal to the rate of gyration of the axis of the vortex ring.

Once the conditions necessary for the establishment of a nearly symmetric bubble were determined, a series of further experiments was performed in order to understand the motion of fluid within and outside the bubble. Another filament was introduced away from the axis of the centre-body and its evolution around the bubble was observed. The upper photo in figure 7 (plate 5) shows that the outer filament remains laminar and relatively unaffected at the section where the central filament finally breaks into turbulence. The lower photo, which was obtained by stopping the injection of the centre dye filament, shows that the outer stream surfaces expand around the bubble and that the flow pattern downstream of the bubble remains visible in spite of the absence of upstream dye injection. In fact, the bubble and the tail configuration remained visible for as long as 20 seconds. The tail configuration could not have remained visible during all that time period had the bubble been closed and had part of the spiralling core downstream of the bubble not been issuing from the bubble. As will be seen later, the tail configuration becomes invisible when the bubble (in a state of growth) is temporarily completely closed.

4. The observations of the travelling vortex breakdowns

A series of experiments was conducted to determine the response of the breakdown to relatively small changes imposed on the *upstream swirling flow*. These changes were produced in various ways: by increasing the inlet flow rate; by

releasing a small air bubble from one of the side vanes; by oscillating one of the vanes; by oscillating the hypodermic tubing used for the eccentric dye injection; and finally, by varying the setting of all vanes.

With a very rapid increase of swirl (increasing vane angle), the bubble first moved (after a measurable time lapse) a short distance (approximately $0{\cdot}2D_0$) downstream and then rapidly upstream, overshooting its final steady-state position by a distance of about $0{\cdot}2D_0$). Then the bubble slowly moved backwards ($\sim 0{\cdot}2D_0$) to its new final position. A rapid decrease of swirl resulted in similar motions in reverse directions.

The diameter of the bubble, which was approximately $0{\cdot}3D_0$ for the steady state, increased rapidly during the downstream motion of the bubble and decreased when the bubble moved upstream. In fact, when the swirl was increased and finally the bubble began to rapidly move upstream, its diameter reduced to about $0{\cdot}2D_0$ and the length of the bubble increased by approximately 30 percent. When the bubble reached its final steady-state form, its length-to-diameter ratio was found to vary between 1·35 and 1·45. The bubble reached its maximum diameter at a distance 67 percent of its length from its front stagnation point.

These experiments clearly demonstrated that the changes imposed on the flow from upstream affect the vortex jump only after a new upstream swirling-flow condition is established and only after the axial velocity of the fluid within the vortex core is modified in accordance with the new swirling flow conditions.

Another series of experiments was conducted to determine the response of the breakdown bubble to relatively small changes imposed on the *downstream flow conditions*. When the flow was *decelerated* by constricting the exit hole at the downstream end of the test tube, the breakdown rapidly *moved upstream* (after a measurable time lapse) and often reached the centre-body in the form of a reversed turbulent core. Figure 8 (plate 6) shows the motion of the bubble relative to the surrounding stream. It is most important to note, by comparing the successive frames in figure 8, that while the bubble propagated considerable distance upstream along the axis of and relative to the surrounding helical coil, *the swirling flow upstream of the bubble remained practically unchanged.* A new upstream swirling-flow condition was set up shortly after the bubble has reached its farthest upstream position. Then, depending on the last position of the bubble, either the same bubble or a new one which emerged near the centre-body moved downstream and came to rest at a point where it would have occurred had the flow been originally set at a rate equal to that of the decelerated flow.

When the downstream flow was *accelerated* by rapidly enlarging the exit hole at the end of the test tube, the bubble rapidly moved *downstream.* Then, after a short time (sufficient for transmission of the 'acceleration information' to the flow at the vanes), either the existing breakdown (if it were not already washed out) began to move upstream (see figure 9, plate 7) and/or a new bubble abruptly came into being upstream of the original position and finally settled at a point where it would have occurred for the new flow rate, had the latter been constant. Under rare circumstances, however, when the rate and duration of the acceleration of the downstream flow were set just right, the original wave rapidly moved upstream and joined the new wave which just came into being

(see figure 10, plate 8). The new breakdown wave (occurring in the region to the left of the vortex-breakdown hysteresis, see figure 12) was, at least initially, *always axisymmetric*. Furthermore, during the period of growth, the bubble was filled with fluid by a perfectly axisymmetric re-entrant jet and there was no partial discharge of flow through a swirling jet as previously described in connexion with stationary breakdowns.

The swelling of the vortex-core filament, disappearance of the dye filament (because of re-entrant jet feeding) immediately downstream of the nascent bubble, and the evolution of a gyrating tail are clearly visible in figure 11 (plate 9). Throughout this process, the outer filament upstream of the bubble remained unaltered whereas the helical filament downstream of the bubble rapidly accommodated the new flow conditions.

5. Measurements

Qualitative observations of the bubble were followed by quantitative measurements of the breakdown location, swirl angle, the axial velocity of the dye front, and the wall-pressure distribution in terms of the flow rate and swirl.

The mean breakdown location was determined by first maintaining the flow rate constant and setting the vane angle at desired values or by maintaining the vane setting and changing the flow rate. In either case, the results did not differ significantly, and the data shown in figure 12 were obtained. Evidently, the type and location of the stationary breakdown are functions of Reynolds and circulation numbers† in the range of Reynolds numbers investigated; for smaller swirls, the axisymmetric breakdown occurs at higher Reynolds numbers; and finally, there is a region along every constant circulation line where there are two stable breakdown conditions, i.e. there is a region of 'vortex breakdown hysteresis'. As the flow rate was slowly increased while maintaining the vane setting fixed, the spiral breakdown moved upstream but maintained its form. Conversely, when the flow rate was slowly decreased in this region, the symmetric breakdown moved downstream.

In the region of hysteresis, both forms (spiral and axisymmetric) were highly unstable and transformed into each other depending on the small disturbances introduced from upstream (abrupt slight increase of vane angle or centre-body motion). A similar hysteresis effect was observed by Lowson (1964) over delta wings with increasing or decreasing incidence in the range of 35° to 45° angle of incidence.

The swirl distribution, a short distance ahead of the breakdown, was determined by injecting dye from the second dye-injection line at various distances away from the surface of the centre-body. The helical streamline and its mirror image were photographed in a manner similar to that described by Harvey (1962) and the data shown in figure 13 were obtained. The swirl angle distribution was found to be a function of the breakdown form. For the axisymmetric form, the

† $Re = U_0 D_0/\nu$ and $\Omega = \Gamma/U_0 D_0$ where U_0 is the mean axial velocity at the entrance to the diverging tube and D_0 (3·81 cm) is the upstream diameter of the diverging tube. For Γ see figure 2.

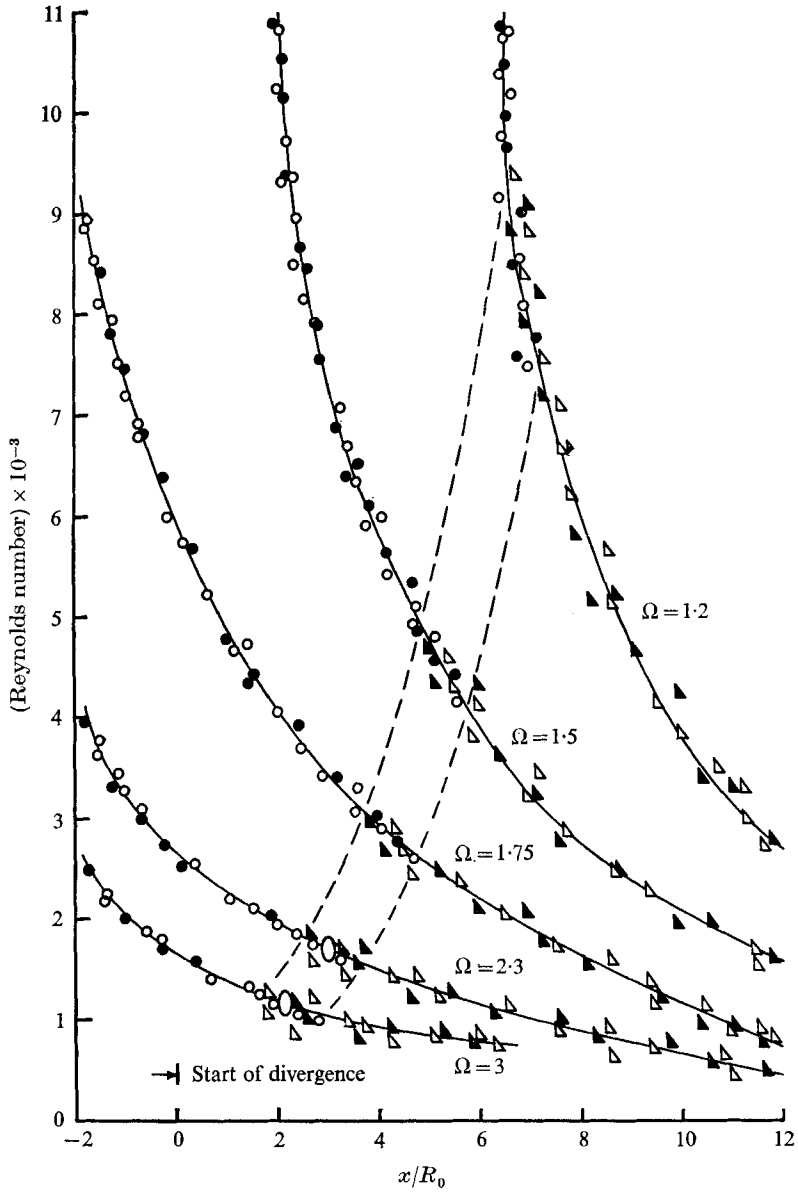

FIGURE 12. Vortex-breakdown position as a function of Reynolds and circulation numbers, ($Re = U_0 D_0/\nu$, $\Omega = \Gamma/U_0 D_0$). ○, axisymmetric breakdown (with fixed vane angle); ●, axisymmetric breakdown (with fixed flow rate); ◺, spiral breakdown (with fixed vane angle); ◣, spiral breakdown (with fixed flow rate). The two ellipses denote the positions of the double-helix vortex breakdowns shown in figure 4. The dotted lines border the region of observed vortex-breakdown hysteresis. x is measured from the start of the diverging tube. The tip of the centre-body is at $x/R_0 = -4{\cdot}50$.

maximum angle was about 50° and independent of the Reynolds and circulation numbers. For spiral breakdown, the maximum swirl angle varied from about 38° to 55°, depending on the intensity of circulation, i.e. in the regions where

spiral breakdown occurred, the total circulation was appreciably less than that where axisymmetric breakdown existed.

The axial velocity of the dye front along the vortex core was determined from the motion pictures by interrupting the dye injection. It was assured that the

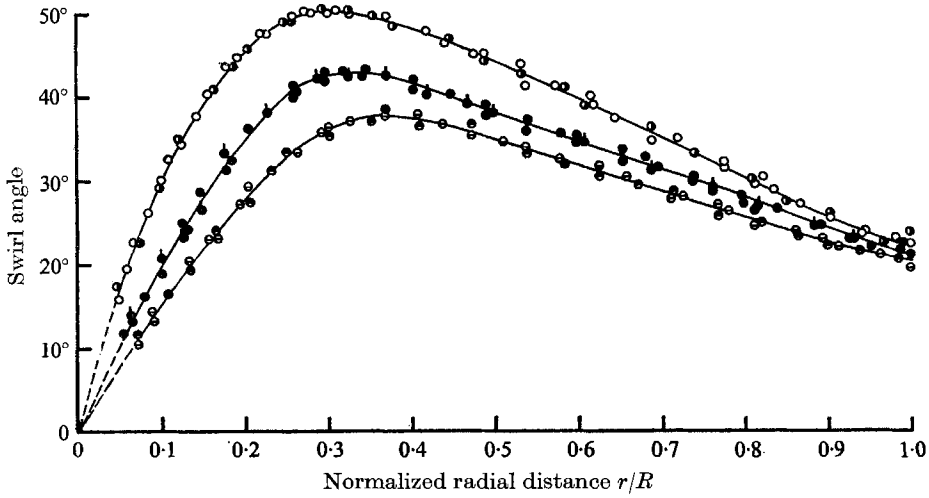

FIGURE 13. Swirl angle distribution. R is the local radius of the tube where the swirl angle is measured. ○, for $Re = 4000$ and $\Omega = 1{\cdot}75$; ◑, for $Re = 7500$ and $\Omega = 1{\cdot}5$; ●, for $Re = 1500$ and $\Omega = 1{\cdot}75$; ◓, for $Re = 4000$ and $\Omega = 1{\cdot}2$; ◭, for $Re = 2200$ and $\Omega = 1{\cdot}75$; and ⊖, for $Re = 6000$ and $\Omega = 1{\cdot}2$.

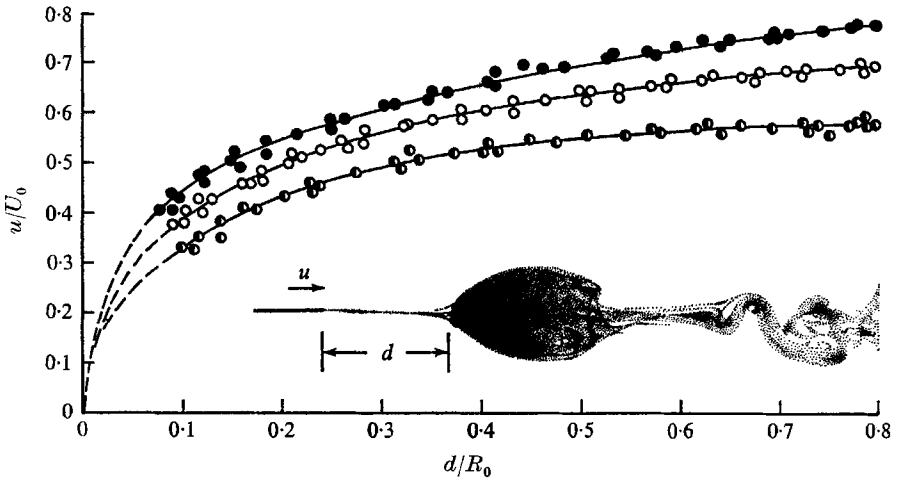

FIGURE 14. The velocity of the vortex-core filament in terms of the relative distance from the bubble. ●, for $Re = 4000$ and $\Omega = 1{\cdot}75$; ○, for $Re = 7500$ and $\Omega = 1{\cdot}5$; and ◐, for $Re = 4000$ and $\Omega = 1{\cdot}2$.

interruption of the dye did not affect the position of the breakdown and that the breakdown was of the perfectly smooth and stable type. The pictures in which the bubble moved (within a time interval of 0·3 sec) were not used in the velocity determination. The representative results are shown in figure 14. The general

trend of the variation of the axial velocity is similar to that predicted by Hall (1966*b*) who has shown that the axial velocity undergoes, for sufficiently large swirls, a pronounced deceleration as a prelude to stagnation both when the bounding stream surface is cylindrical and when it expands. It is not possible at this stage to make an accurate comparison between the experimental results presented herein and Hall's predictions since the initial and boundary conditions assumed by Hall are, as has been pointed out by him, to a certain extent arbitrary and the numerical method employed is strictly applicable to laminar flows only.

Representative wall pressure distributions are shown in figure 15. As previously observed by Kirkpatrick (1964), there is a slight positive pressure gradient upstream of the breakdown and a negative gradient immediately downstream.

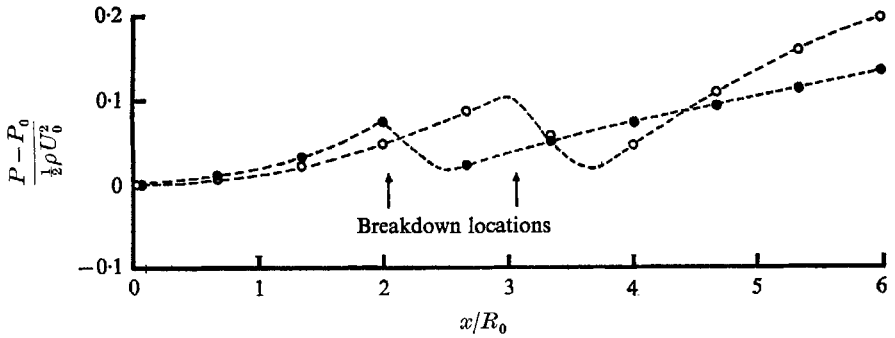

FIGURE 15. Representative wall-pressure distributions. P_0 denotes the pressure at the start of the diverging tube. ○, for $Re = 7500$ and $\Omega = 1{\cdot}5$; and ●, for $Re = 4000$ and $\Omega = 1{\cdot}75$.

6. Résumé of findings

(i) There are three basic types of stationary vortex breakdown, viz. double helix, spiral, and axisymmetric. The vortex core filament spirals in or around each form. The type and the shape of the intermediate forms depend upon the particular combination of the Reynolds and circulation numbers.

(ii) The swirling flow is highly unstable to spiral disturbances for Reynolds numbers between approximately 1000 and 2000. In this region, either mode of transition (single or double spiral) may be observed.

(iii) There is a second region fairly well defined by certain values of Reynolds and circulation numbers (the right side of the hysteresis region) in which only the spiralling type of breakdown occurs. The experiments in this region could not yet establish as to whether the growth of the disturbances gave rise to spiral core or the finite-transition waves caused the temporally periodic motion.

(iv) The axisymmetric breakdown evolves either from a double helix, or from a spiral, or directly from an axisymmetric swelling of the vortex core. The mode of evolution depends on the particular region defined by the Reynolds and circulation numbers. For sufficiently high Reynolds and circulation numbers (the left side of the hysteresis region) the axisymmetric bubble evolves only from a symmetric swelling of the vortex core, enclosing an ovoid region of circulating

fluid. Instabilities in the wake of the bubble render the motion unsteady and only the rudiments of a wave train can be observed. The formation of the bubble in this region is not preceded by the amplification of travelling-wave disturbances in the usual manner of hydrodynamic instabilities.

(v) The response of the axisymmetric-form to changes imposed on the upstream or downstream flow conditions is analogous to that of a hydraulic jump between two sequent states of flow. The constricting effect of the tube wall and the swirling nature of flow prevent a precise identification of the corresponding physical features of the two flows. Nevertheless, the finite-transition concept proposed by Benjamin (1962) is wholly in accord with the observations made in the axisymmetric breakdown region.

(vi) The observations reported and the evidence presented suggest that the vortex-breakdown phenomenon is governed by two basic and conceptually different mechanisms: hydrodynamic instability and finite-transition to a sequent state. Which mechanism will bring it about depends on the particular combination of the Reynolds and circulation numbers of the flow. Instability manifests itself more emphatically at low Reynolds and high circulation numbers. The finite-transition type of behaviour of the axisymmetric breakdown is brought out more clearly in an unsteady swirling flow (such as the one created by the perturbation of circulation) than in a swirling steady flow.

(vii) No simple explanation can be offered regarding the difference in the sense of rotation of the spiral breakdown relative to that of the ambient flow in a tube and a leading-edge vortex.

(viii) The static pressure variation along the wall of the tube yields no new information other than that already revealed by the measurements of Kirkpatrick (1964). It may become important in checking the results of theoretical calculations.

This research has been partially supported by the Office of Naval Research. The author cannot adequately acknowledge all who have helped to germinate the ideas which have resulted in the present paper but would like to appreciatively mention N. C. Lambourne, T. Brooke Benjamin, and M. G. Hall, and to apologize to those whom he has omitted. Thanks are also due to Lt. L. E. Rodriguez and Lt. M. L. McHugh for their assistance with the experiments. The constructive comments of the reviewers on the first draft of this paper are sincerely appreciated.

REFERENCES

BENJAMIN, T. B. 1962 Theory of the vortex breakdown phenomenon *J. Fluid Mech.* **14**, 593.

BENJAMIN, T. B. 1965 Significance of the vortex breakdown phenomenon. *Trans. Am. Soc. Mech. Engrs, J. Basic Engng* **87**, 518 and 1091.

BENJAMIN, T. B. 1967 Some developments in the theory of vortex breakdown. *J. Fluid Mech.* **28**, 65.

GRANGER, R. A. 1968 Speed of a surge in a bathtub vortex. *J. Fluid Mech.* **34**, 651.

HALL, M. G. 1966*a* The structure of concentrated vortex cores. In *Progress in Aeronautical Sciences*, **7** (ed. D. Küchemann *et al.*). Pergamon.

HALL, M. G. 1966*b* On the occurrence and identification of vortex breakdown. *R.A.E. Tech. Report* no. 66283.

HARVEY, J. K. 1962 Some observations of the vortex breakdown phenomenon. *J. Fluid Mech.* **14**, 585.

JONES, J. P. 1960 The breakdown of vortices in separated flow. *University of Southampton U.S.A.A. Report* no. 140.

JONES, J. P. 1964 On the explanation of vortex breakdown. *IUTAM Symposium on Vortex Motions*. Ann Arbor.

KIRKPATRICK, D. L. I. 1964 Experimental investigation of the breakdown of a vortex in a tube. *R.A.E. Tech. Note* no. Aero 2963.

LAMBOURNE, N. C. 1965 The breakdown of certain types of vortex. *N.P.L. Aero Report* 1166.

LAMBOURNE, N. C. & BRYER, D. W. 1962 The bursting of leading edge vortices—some observations and discussion of the phenomenon. *Aero. Res. Counc. R & M* 3282.

LUDWIEG, H. 1962 Zur Erklärung der Instabilität der über angestellten Deltaflügeln aufteten freien Wirkbelkerne. *Z. Flugwiss.* **10**, 242.

LUDWEIG, H. 1964 Explanation of vortex breakdown by the stability theory for spiralling flows. *IUTAM Symposium on Vortex Motions*, Ann Arbor. Available as AVA-Bericht 64 A 14.

LOWSON, M. V. 1964 Some experiments with vortex breakdown. *J. Roy. Aero. Soc.* **68**, 343.

PRITCHARD, W. G. 1970 Solitary waves in rotating fluids. *J. Fluid Mech.* **42**, 61.

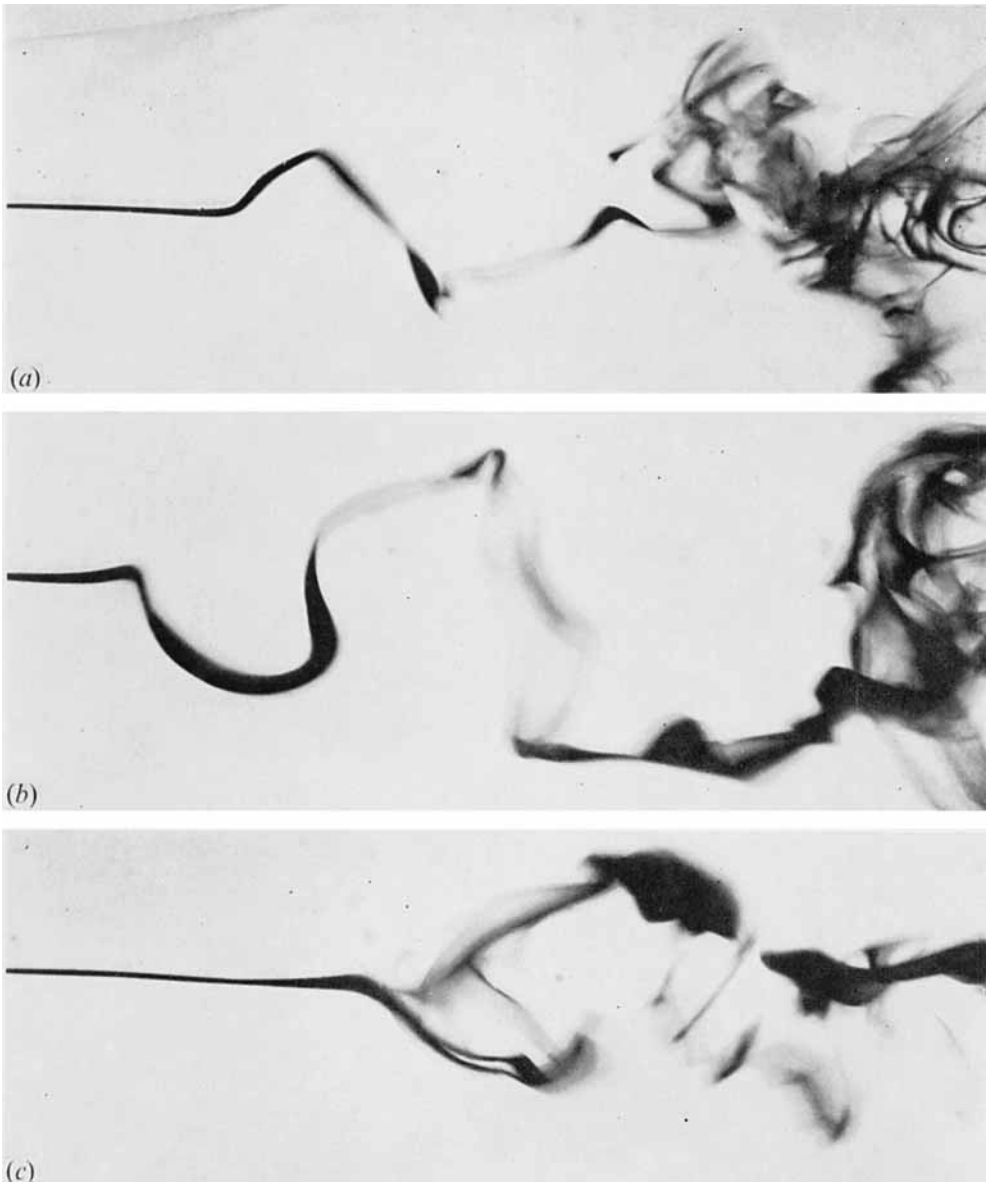

FIGURE 3. (*a*) Initiation of the spiral vortex breakdown, (*b*) spiral breakdown prior to the inception of bubble, and (*c*) the nascent state of the axisymmetric vortex breakdown.

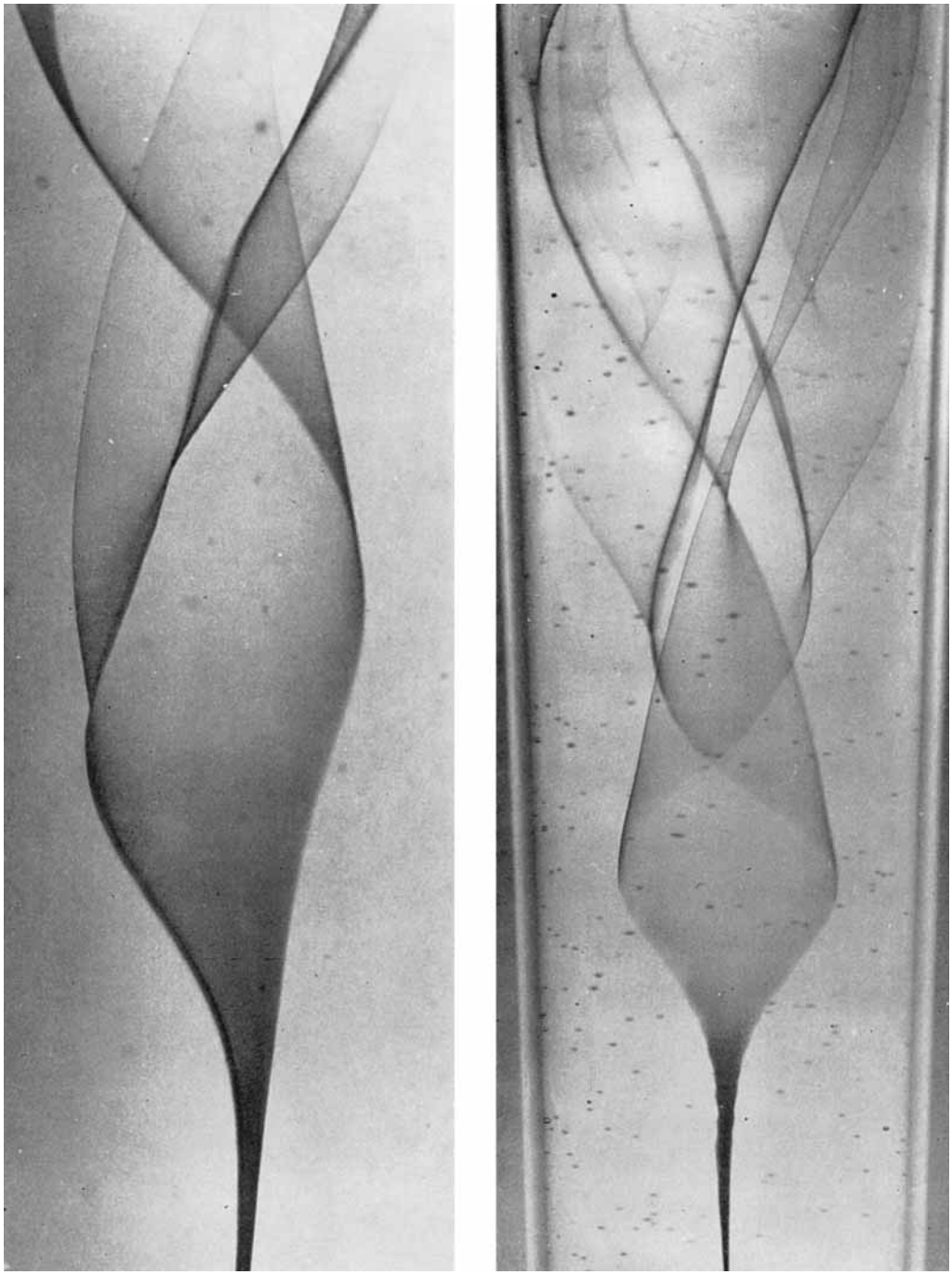

FIGURE 4. Double-helix vortex breakdowns. Top picture for $Re = 1150$, $\Omega = 3$ and bottom picture for $Re = 1700$, $\Omega = 2{\cdot}3$.

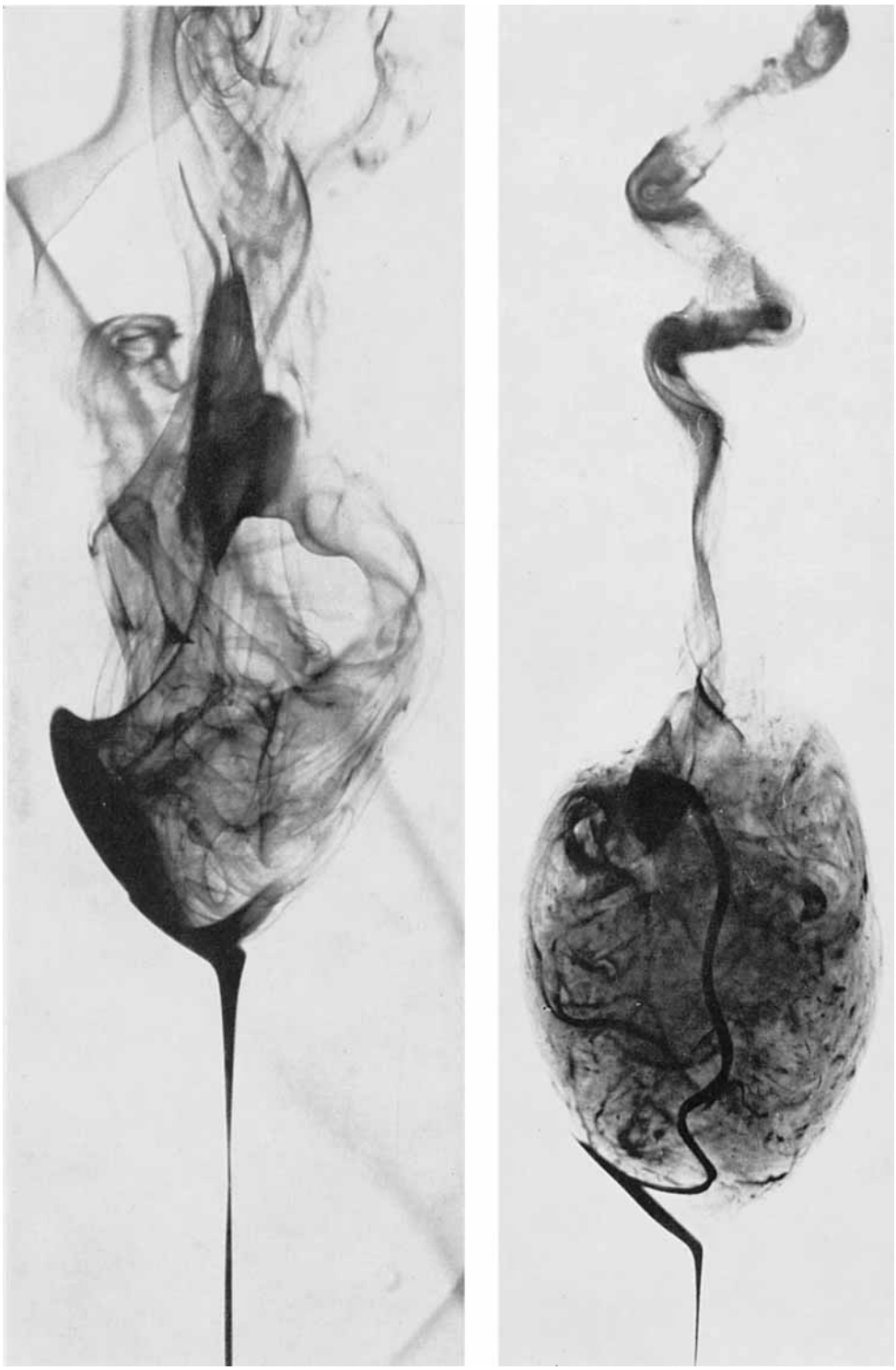

FIGURE 5. Top picture: An unstable bubble in the hysteresis region. Bottom picture: The spiralling of the vortex core in and around the bubble. The inclined vortex-ring, the path of the dye-filament near the wake, and the unsymmetry of the wake clearly show the filling and emptying of the bubble. This picture was taken shortly after the dye filament was interrupted.

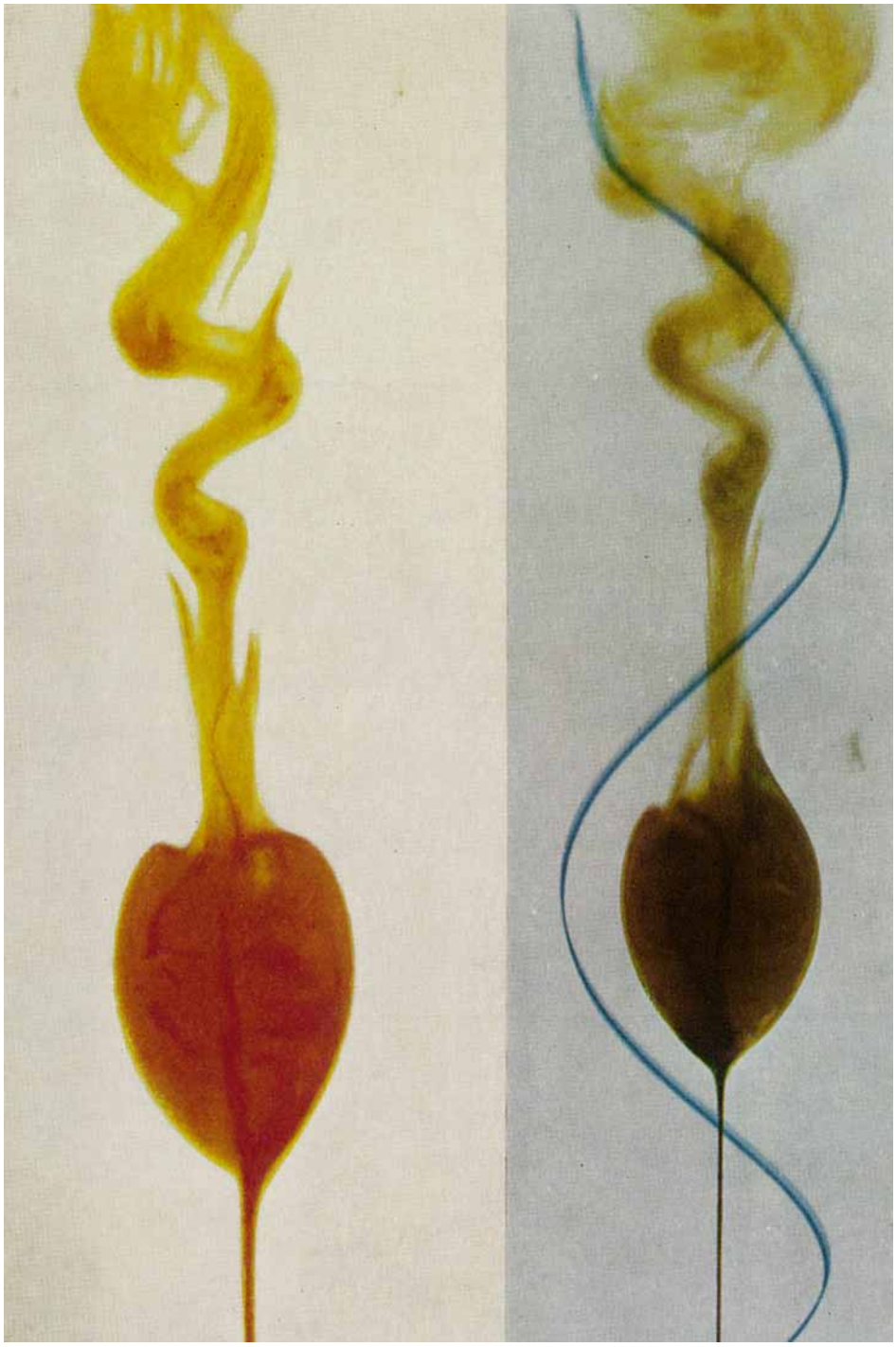

FIGURE 6. Representative, nearly axisymmetric, vortex breakdowns. The lower photograph shows the wake instability, the filling and emptying of the bubble, and the change of the swirl angle as the flow changes from supercritical to subcritical state.

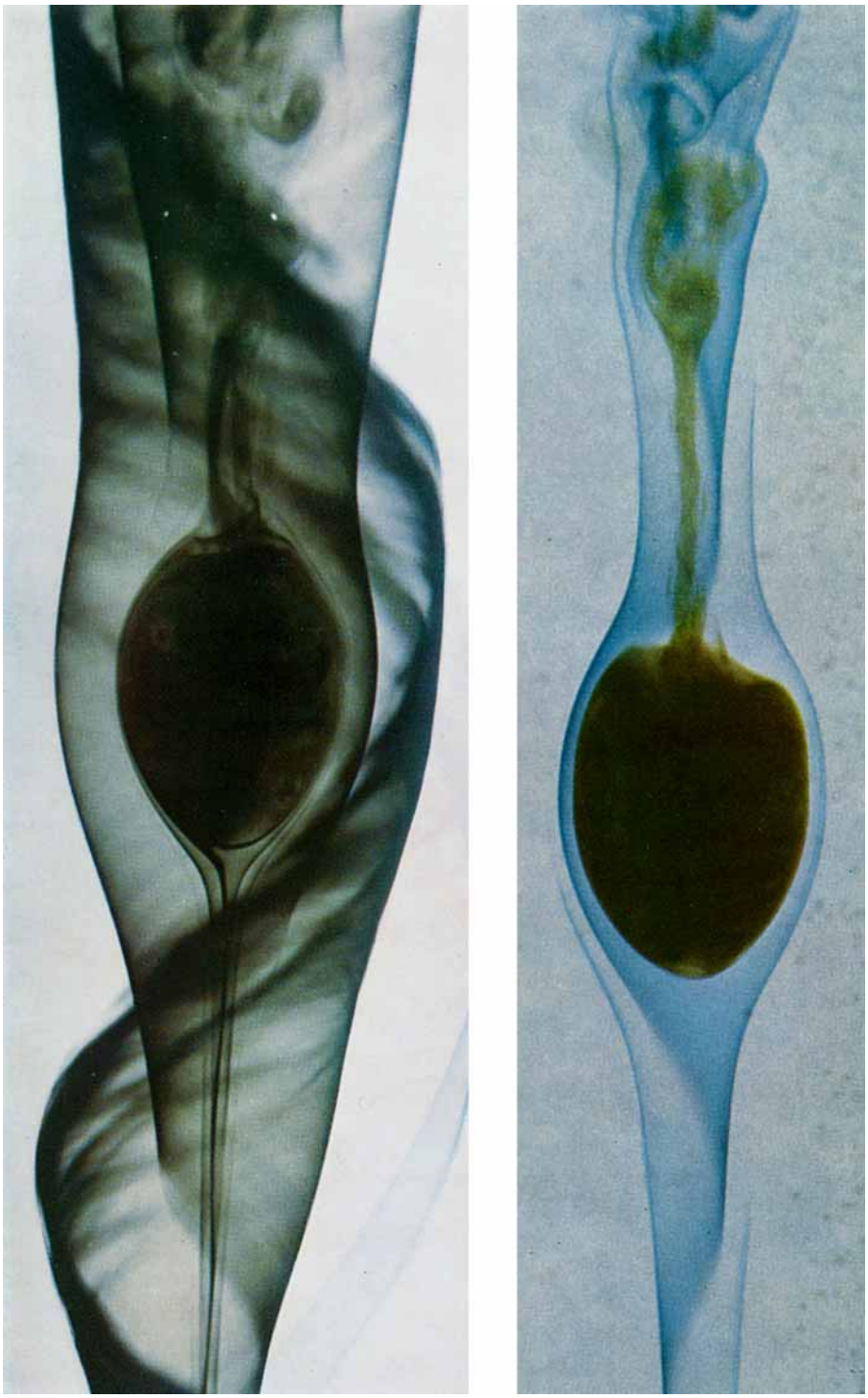

FIGURE 7. Upper photograph shows that the outer filament remains laminar and relatively unaffected at the section where the central filament finally breaks into turbulence. Both the upper and lower pictures show that the outer stream surfaces expand around the bubble.

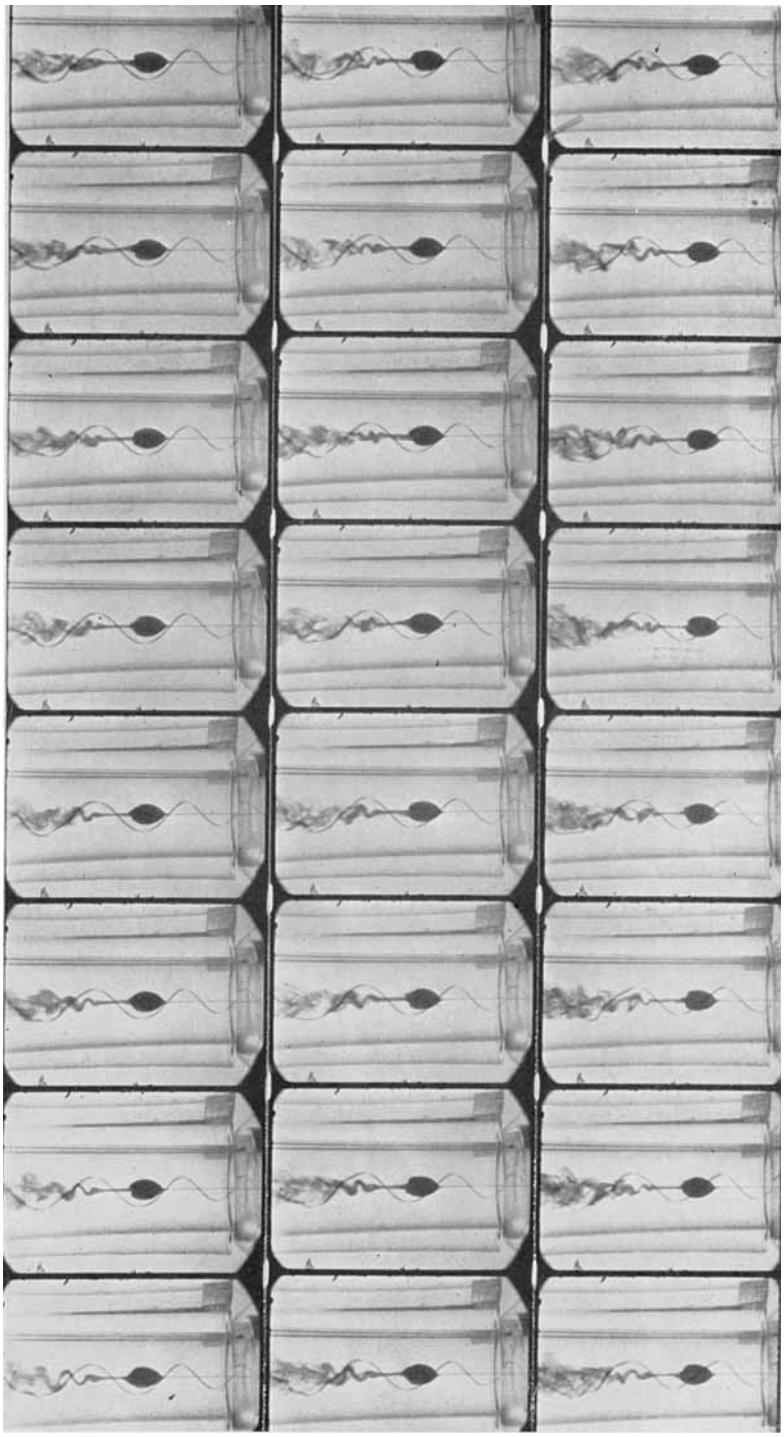

FIGURE 8. The motion of the bubble relative to the surrounding stream. The motion picture was taken shortly after the flow was decelerated by constricting the exit hole at the downstream end of the test tube. Frames follow from top to bottom starting at the upper left-hand corner. It should be noted that the flow ahead of the bubble remains unaffected. The change of the swirl angle, evolution of the wake, and the gyration of the new core are clearly visible. The film speed was 16 frames/sec.

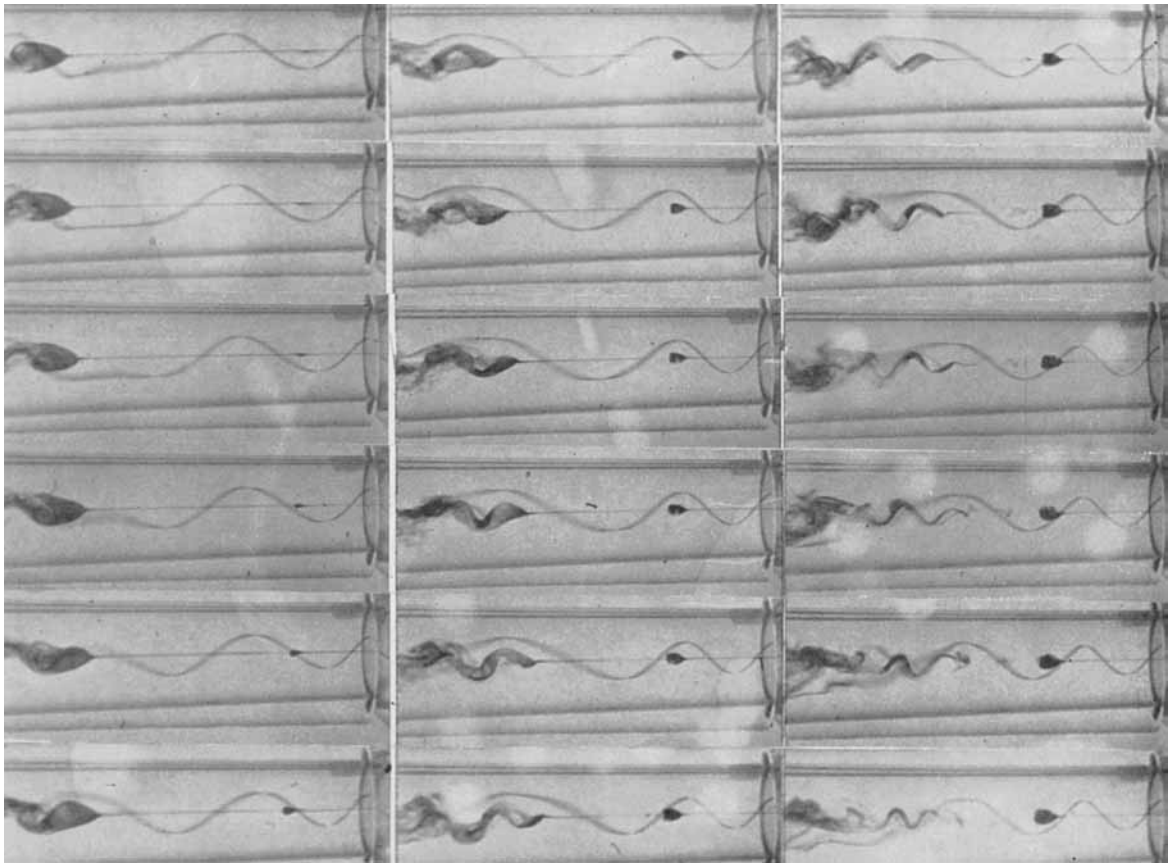

FIGURE 9. The birth and growth of a bubble and the propagation upstream of a travelling breakdown. The axial symmetry of the initial disturbance, the evolution of the streamlines between the two disturbances, and the inability of the waves to propagate into the supercritical flow are clearly visible.

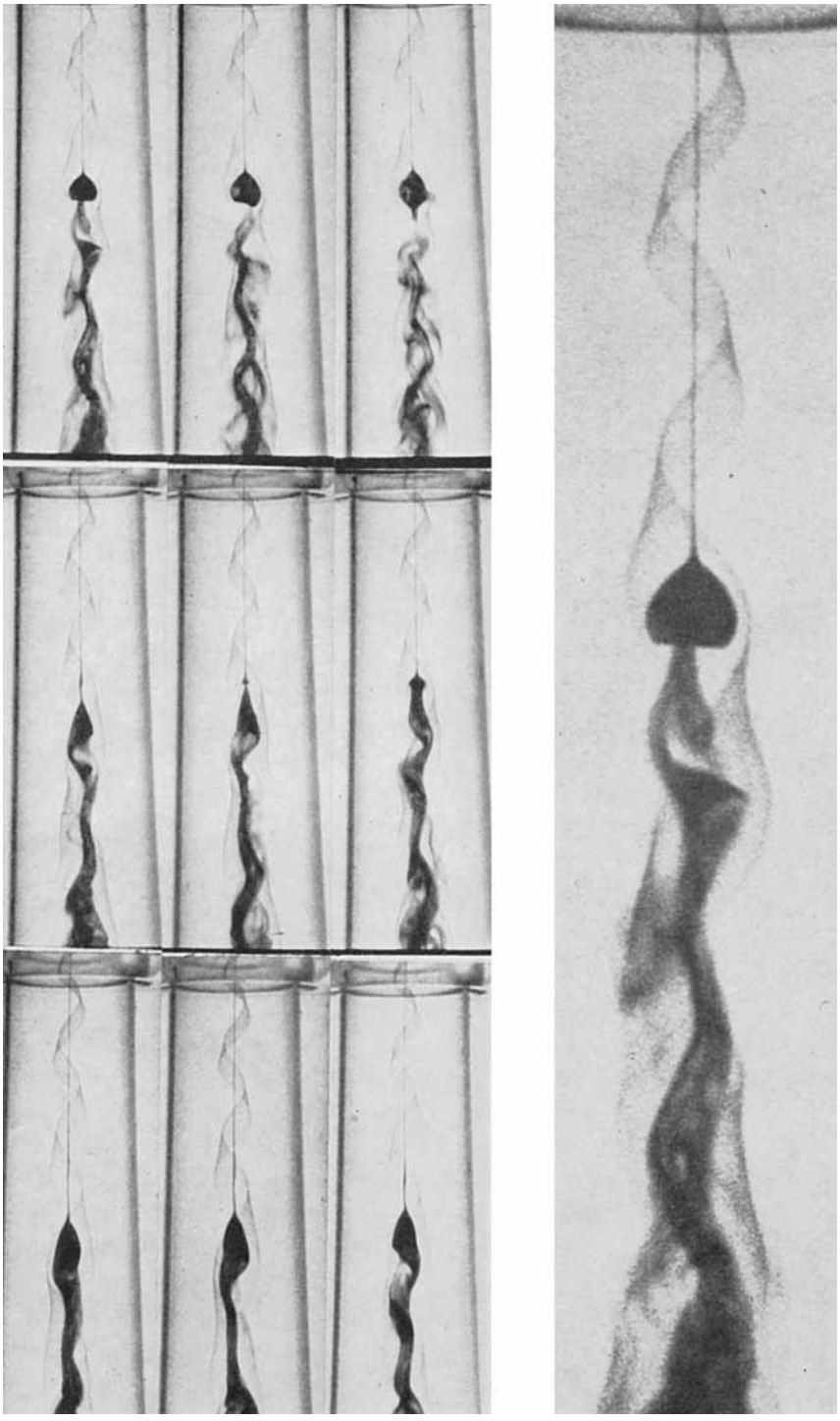

FIGURE 10. The birth of a bubble and the propagation upstream of an existing breakdown. These pictures show that the flow between the new and the old wave rapidly transforms into a subcritical state, the new breakdown is axisymmetric at birth, and that there are no waves or disturbances in the supercritical flow upstream of the new bubble. The lower photo shows the rudiments of a wave train.

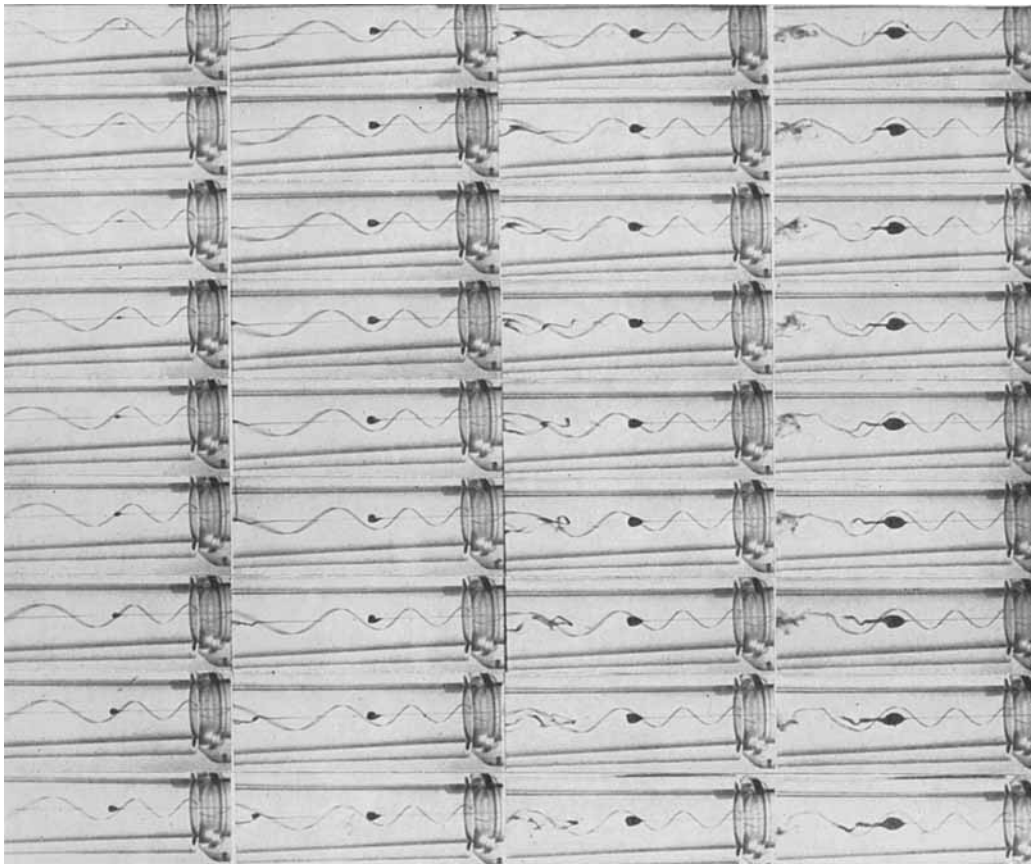

FIGURE 11. This picture shows the swelling of the vortex-core filament, disappearance of the dye filament immediately downstream of the bubble, and the evolution of a gyrating tail. Frames follow from top to bottom starting at the upper left hand corner. The film speed is 16 frames/sec.